Published in final edited form as:
Pediatr Nephrol. 2012 March ; 27(3): 469–483. doi:10.1007/s00467-011-2001-z.

Role of circulating Fibroblast Growth Factor-2 in lipopolysaccharide-induced acute kidney injury in mice

Parnell C. Mattison, **Ángel A. Soler-García**, **Jharna R. Das**, **Marina Jerebtsova**, **Sofia Perazzo**, **Pingtao Tang**, and **Patricio E. Ray***
Division of Nephrology, Center for Molecular Physiology Research, Children's National Medical Center, and Department of Pediatrics, The George Washington University, Washington, DC, USA

Abstract

Background—Fibroblast Growth Factor (FGF-2) is an angiogenic growth factor involved in renal growth and regeneration. Previous studies in rodents showed that single intrarenal injections of FGF-2 improved the outcome of acute kidney injury (AKI). Septic children usually show elevated plasma levels of FGF-2, and are at risk of developing AKI. However, the role of circulating FGF-2 in the pathogenesis of AKI is not well understood.

Methods—Here, we developed a mouse model to determine how FGF-2 released into the circulation modulates the outcome of AKI induced by lipopolysaccharide (LPS). Young FVB/N mice were infected with adenoviruses carrying a secreted form of human FGF-2 or control *LacZ* vectors. Subsequently, when the circulating levels of FGF-2 were similar to those seen in septic children, mice were injected with a non-lethal dose of LPS or control buffer.

Results—All mice injected with LPS developed hypotension and AKI, and recovered after five days. FGF-2 did not improve the outcome of AKI, and induced more significant renal proliferative and apoptotic changes during the recovery phase.

Conclusions—These findings suggest that circulating FGF-2 may not necessarily prevent the development or improve the outcome of AKI. Moreover, the renal accumulation of FGF-2 might cause further renal damage.

Keywords

Acute kidney injury; FGF-2; NGAL; urinary biomarkers; mouse model; LPS

Introduction

Acute kidney injury (AKI) is a common clinical entity in children admitted to pediatric intensive care units [1]. This complication usually occurs as a secondary outcome of systemic infections caused by Gram-negative bacteria that induce endotoxic shock, and is associated with high mortality rates [1-4]. Gram-negative bacteria synthesize lipopolysaccharide (LPS), which is a major constituent of their outer cell membranes [3, 4]. When LPS is released from the cell membrane, it causes a significant inflammatory response characterized by the recruitment of activated neutrophils, monocytes, macrophages, and induction of endothelial damage [2-4]. All these changes cause poor renal perfusion and hypoxia, leading to the development of acute tubular necrosis [3, 4].

*Corresponding author.: Patricio Ray, Room 5346, 5th floor, Children's National Medical Center, 111 Michigan Avenue NW, Washington, DC 20010. Phone: (202) 476-2912, Fax: (202) 476-4477, Pray@cnmc.org.

Many cytokines released by inflammatory cells play a critical role in the pathogenesis of sepsis-induced acute kidney injury (AKI) [2-4]. Among them, Tumor Necrosis Factor alpha (TNF-) is a critical mediator of LPS-induced cytotoxic effects [3, 4]. An interesting report previously found that LPS induced generalized apoptosis of mouse microvascular endothelial cells through the release of TNF- and the generation of ceramide [5]. Moreover, this study found that FGF-2, given intravenously concomitant with the LPS injection, decreased the number of endothelial cells undergoing apoptosis and improved the survival of these mice [5]. However, other studies have questioned the notion that LPS induced disseminated endothelial cell apoptosis in mice [6], and it is unclear how LPS and FGF-2 modulate the behavior of renal endothelial cells *in vivo*. Nevertheless, since renal endothelial dysfunction can contribute to the pathogenesis of AKI induced by LPS [7], and FGF-2 is a well known survival factor for endothelial cells [8], it is possible that FGF-2 may improve the renal outcome of mice exposed to LPS by preventing endothelial injury.

In addition to its angiogenic activity, FGF-2 is also considered a powerful renal tubular regenerative growth factor [9, 10]. Previous studies showed that one single intrarenal injection of FGF-2, given simultaneously during the induction of acute renal ischemic injury, accelerated the regeneration and recovery of renal tubules in rats [11, 12]. However, other studies in human and rodents showed that the renal accumulation of FGF-2 can cause tubular proliferative and fibrogenic lesions [13-16]. Children admitted to pediatric intensive care units with endotoxemia frequently show elevated plasma levels of FGF-2 [17, 18], and are at risk of developing AKI. To date, it is unclear how FGF-2 released into the circulation of these patients may affect their renal outcome. Therefore, we developed a mouse model system to explore the role of circulating FGF-2 in the pathogenesis of AKI induced by LPS. We found that circulating FGF-2 did not prevent or accelerate the renal recovery of LPS-treated mice, and could potentially cause further renal damage.

Methods

Experimental design

All experiments were approved by the Children's Research Institute Animal Care and Use Committee. FVB/N male mice (8 weeks old, 25-30 grams) were purchased from Jackson Laboratory (Bar Harbor, ME), and housed in a pathogen-free environment, 12:12-h light-dark cycle, in our animal facility. All mice received food and water ad libitum. Mice of were divided in two similar groups (n = 26 mice per group), and injected with recombinant adenoviral (rAd) vectors carrying the *Escherichia coli LacZ* gene (rAd-*LacZ* control vector) or rAd vectors carrying a 700-bp cDNA sequence encoding a secreted form of human FGF-2 (rAd-FGF-2 vector), as previously described [19]. Two days after the injection of the adenoviral vectors, 13 mice in each group were injected intraperitoneally with 90 μg/mouse LPS (*Esherichia coli*, 0127:B8, Sigma, St. Louis, MO), resuspended in 100 l pyrogen-free phosphate buffered saline (PBS). The remaining 13 mice in each group were injected with 100 l PBS alone (PBS controls). Mice were sacrificed at specific time points, 6 hours, 2 days, and 5 days after the LPS or PBS injections (n = 3 - 5 mice per group).

Adenoviral vectors

The adenoviral vectors were generated, amplified, and purified as previously described [20, 21]. The particle-to-plaque-forming unit (pfu) ratio of the virus stock used in these experiments was 100. Mice were injected via the retro-orbital vein plexus with 5×10^8 pfu/mouse of either rAd vector, as described before [22]. Blood samples were taken in four mice 72 hours after the injection of adenoviral vectors, to assess the plasma levels of FGF- 2 by ELISA (R&D kit. Minneapolis, MN), as previously described [22].

Non-invasive blood pressure monitoring

Systolic blood pressure was measured with an automated tail-cuff device (BP-2000, Visitech Systems, Apex, NC) as described previously [23]. Mice were trained before the blood pressure was taken. Subsequently, the final blood pressure monitoring was completed at baseline and at 6 hours, 2 days, and 5 days after the LPS/PBS injections.

Blood and urine sample collection

Mice were anesthetized with inhaled isoflurane. Blood samples were drawn from the retro-orbital vein plexus, collected in heparin-coated Eppendorff tubes and centrifuged at 1,800 rpm for 10 minutes. Blood Urea Nitrogen was assessed using the Quantichrom Urea Assay Kit from BioAssay Systems (Hayward, CA) as described before [24]. Serum creatinine was measured using a modification of the kinetic Jaffe reaction using the Dade Behring Dimensional RXL chemistry analyzer from Siemens Healthcare Diagnosis (Deerfield, IL). Proteinuria was measured using the Bayer Multistix 10 SG reagent strips for urinalysis. To detect albuminuria, five microliters of urine were also run on 10% sodium dodecyl sulfate polyacrylamide gel electrophoresis (SDS-PAGE) and stained with Coomassie Blue Stain Solution (Bio-Rad, Hercules, CA). Protein bands corresponding to albumin were quantified by densitometric analysis using Adobe Photoshop 6.0. Results were expressed in arbitrary optical density units adjusted to the urinary creatinine and baseline control values.

Enzyme-linked immunosorbent assay (ELISA) to assess the urinary levels of Neutrophil Gelatinase-Associated Lipocalin (NGAL)

The urinary NGAL ELISA was performed as previously described using anti-mouse antibodies and recombinant protein (R & D Systems) [25]. Mouse urinary NGAL concentrations were determined in 50 l urine samples tested in duplicate by comparison against a standard curve of recombinant mouse NGAL. Urine creatinine was measured colorimetrically using the Creatinine Parameter assay kit as described before (R& D Systems) [24]. The urinary NGAL concentration was expressed as a ratio of the urinary creatinine (ng/mg).

Western blot analysis

The kidneys were harvested and homogenized using RIPA lysis buffer containing protease inhibitors and phosphatase inhibitor cocktail 2, purchased from Sigma-Aldrich (St. Louis, MO). The protein concentration in these samples was measured using the BCA Protein assay kit (Thermo Scientific, Inc., Rockford, IL) and bovine serum albumin as standard. Equal amounts of protein (10-30 μg) were loaded onto 4-16% Bis-Tris gel (Invitrogen Corporation, Carlsba, CA), and then transferred to nitrocellulose membranes (0.2 μm, from Bio-Rad). The membranes were probed with primary antibodies: Phospo-p44/42 MAP kinase (Thr202/Tyr204) (Catalog No.9101) p44/42 MAP kinase (Catalog No.9102), obtained from Cell Signaling Technology (Boston, MA); Proliferating cell nuclear antigen (PCNA) (C-20) rabbit polyclonal, (Catalog No. SC-9857); Caspase-3 (Pro and Active) rabbit polyclonal antibody, (Catalog No.SC-7148), obtained from Santa Cruz Biotechnology, Inc. (Santa Cruz, CA). Beta-Actin (AC-15) mouse monoclonal, (Catalog No.A1978) obtained from Sigma- Aldrich, St. Louis, MO. All primary antibodies were diluted 1:1000 and incubated overnight at 4°C. Then membranes were washed five times and incubated for 1 hour at room temperature with the corresponding horseradish peroxidase-conjugated secondary antibodies, goat antirabbit IgG-HRP, (catalog No. 170-6515); and goat anti-mouse IgG-HRP, (Catalog No.170- 6516) obtained from Bio-Rad., at 1:5,00 dilution. Subsequently the membranes were washed five times and the detection of the corresponding antibodies was done using the Supersignal West Pico Chemiluminescent Substrate, from Thermo Scientific, according to the manufacturer's instruction. All

membranes were then exposed to a Kodak film (X-OMAT) from Kodak Scientific Imaging and developed using automated developer. Densitometric analysis was conducted using Adobe Photoshop 6.0.

Immunohistochemistry

Paraffin embedded sections were cut at 5 m, deparaffinized, rehydrated, and stained with hematoxylin and eosin or Masson's trichrome as previously described [22]. For immunohistochemistry studies, the renal sections were heated twice for five minutes each in 0.01mol/L sodium citrate (pH 6.0) in a microwave oven (2450 mHz, 850 W) to augment antigen retrieval. Endogenous peroxidase activity was blocked by treating with 3% H_2O_2 in 100% methanol for 10 minutes. Immunostaining was performed with a commercial streptavidin-biotin-peroxidase complex Histostain SP kit (Zymed, San Francisco, CA) according to the manufacturer's instructions, as described before [22]. The peroxidase substrate chromogen was aminoethyl carbazole. Sections were counterstained with hematoxylin. PCNA was detected with the PCNA staining kit from Invitrogen (Cat # 93-1143). The phospho- p44/42 MAPK (pERK) staining was assessed using a 1:75 dilution of the rabbit anti-pERK antibody from Cell Signaling (#9101); alpha-smooth muscle actin staining was detected using 1:200 dilution of a mouse anti alpha-actin antibody (Sigma A-2547). The renal recruitment of macrophages was detected with a rat anti-mouse F4/80 antibody (Clone CIA3-1) purchased from AbD Serotec (Raleigh, NC). The CD34 staining was done using the rat anti-mouse CD34 IgG antibody (1:200 dilution) from Cedarline Laboratories USA Inc., (Burlington, NC). For CD34 antigen unmasking, renal tissues were treated with 0.4% Pepsin (Sigma) in 0.2 N HCl for 20 minutes at 37°C. Controls included replacing the primary antibody with equivalent concentrations of the corresponding non-specific antibodies and/or omitting the first or second antibodies. Apoptosis was assessed using the Apop Tag *in situ* apoptosis detection kit (Oncor, Gaithersburg, MD), which is based on the Terminal Deoxynucleotidyl Transferase-mediated dUTP Nick-End Labeling (TUNEL) method, according to the manufacturer's instructions. The intensity and localization of the staning was assessed by two investigators, and quantified as previously described [19].

Statistical analysis

Results are expressed as mean + SD. Differences between two groups were compared by the Student's t-test. When more than two means were compared, differences were measured by one-way analysis of variance followed by multiples comparison using the Student-Neuman-Keul test. In addition, the nonparametric Kruskal-Walls test was used to analyze small sample size groups ($N < 5$). However, since the mean and the median of these groups did not differ by much, results were expressed in terms of mean + SD. p values of less than 0.05 were considered significant.

Results

Reversible model of acute kidney injury in LPS-treated mice infected with LacZ or FGF-2 adenoviral vectors

To determine how FGF-2 affected the cytotoxic effects of LPS in the kidney, five mice in each group were sacrificed six hours, two days, and five days after the LPS injections (Fig. 1A-B). Before the LPS injection, mice infected with rAd-FGF-2 vectors showed elevated plasma levels of FGF-2 (117 + 48 pg/ml), which is consistent with the values reported in septic children [26]. Human FGF-2 was not detected in the circulation of mice injected with rAd-*LacZ* vectors. Control mice infected with rAd-*LacZ* or rAd-FGF-2 vectors and injected with PBS did not develop significant renal injury (Fig 1A-B). After the LPS injection, all mice injected with LPS developed a reversible form of acute kidney injury (Fig. 1A-B).

LPS-induced renal functional changes

Before the LPS injection, no significant changes in renal function were detected in mice infected with rAd-*LacZ* or rAd-FGF-2 (Fig. 1A, a-c). Six hours after the LPS injection, the BUN levels increased in both groups, reaching higher values in mice infected with rAd-*LacZ* vectors (61.1 ± 1.3* vs. 48.5 ± 2.7 mg/dL, for Ad-*LacZ* and rAd-FGF-2 infected mice, respectively; * $p < 0.05$) (Fig. 1A, a). Subsequently, the BUN levels continued to rise, but two days after the LPS injection, the highest BUN levels were seen in mice infected with rAd-FGF-2 (121.9 ± 7.0* mg/dL vs. 93.6 ± 4.2, for rA-FGF-2 vs. rAd- *LacZ* infected mice, respectively; n =5; *$p < 0.05$) (Fig. 1A, a). Finally, the BUN levels decreased in both groups, reaching almost normal values five days after the LPS injection, in correlation with their clinical recovery (32.8 +3.0 vs. 35.3 ± 2.4 mg/dL, for rAd-*LacZ* vs rAd- FGF-2 infected mice, respectively (n = 5; $p > 0.05$) (Fig. 1A, a). In agreement with previous studies [27, 28], the serum creatinine levels were not a sensitive early marker of AKI in LPS-treated mice. Six hours after the LPS injection, no statistically significant changes in the serum creatinine levels were detected between control and LPS treated mice (0.25 ± 0.03 vs. 0.31 ± 0.04 and 0.34 ± 0.02 mg/dL, for rAd-*LacZ* + PBS vs. rAd-*LacZ* or rAd-FGF-2 + LPS treated mice, respectively; n = 5; $p > 0.05$) (Fig. 1A, b). In contrast, two days after the LPS injection, the serum creatinine levels increased in a significant manner in all mice injected with LPS (0.27 ± 0.04 vs. 0.48 ± 0.03* and 0.5 ± 0.02* mg/dL, for control rAd-*LacZ* ± PBS mice vs. rAd-*LacZ* + LPS, and rAd-FGF-2 + LPS mice, respectively; n = 5 * $p < 0.05$) (Fig. 1A, b). Finally, five days after the LPS injection, the serum creatinine levels returned to normal values in all mice (Fig. 1A, b).

The urinary levels of NGAL were measured as an additional marker of AKI (Fig. 1A, c)**.** Six hours after the LPS injection, urinary NGAL was elevated in all mice treated with LPS (188.9 ± 22.1 vs 192.8 ± 27.2 ng/mg of creatinine, for rAd-*LacZ* and rAd-FGF-2 groups, respectively) (Fig. 1A, c). Urinary NGAL levels remained elevated throughout the follow up period, but decreased from the six hours value by 34% and 37% two days after the LPS injection, and returned to almost normal values by five days (Fig. 1A, c). No significant statistical differences in the urinary NGAL levels were detected between LPS-treated mice infected rAd-*LacZ* or rAd-FGF-2 vectors, at any time point.

Before the LPS injection, no significant differences in albuminuria were found between mice infected with rAd-*LacZ* or rAd-FGF-2 vectors (Fig. 1A, d). As shown in a previous study [29], mice injected with LPS developed transient albuminuria. These changes peaked at six hours after the LPS injection, and returned to almost normal values after five days (Fig. 1A, d). No significant differences in albuminuria were detected between LPS-treated mice infected with rAd-*LacZ* or rAd-FGF-2 vectors, at any time point (Fig. 1A, d).

LPS-induced changes in systolic blood pressure

Before the LPS injection, mice infected with rAd-*LacZ* and rAd-FGF-2 showed normal blood pressure values (117.0 ± 6.3 vs 126.7 ± 7.6 mm Hg, for rAd-*LacZ* and rAd-FGF-2 infected mice respectively; n = 5, $p > 0.05$). Their blood pressure remained undetectable six hours and two days after the LPS injection. Finally, the systolic blood pressure returned to normal values five days after the LPS injection (118.7 ± 7.5 vs 124.0 ± 5.9 mm Hg, for rAd-*LacZ* and rAd-FGF-2 infected mice, respectively; n = 5, $p > 0.05$).

LPS-induced renal histological injury

Before the LPS injection, no significant renal histological lesions were detected by light microscopy in mice infected with rAd-*LacZ* or rAd- FGF-2 vectors (Fig. 1B, a, e). In contrast, after the LPS injection, renal sections harvested from mice infected with rAd-*LacZ* or rAd-FGF-2 vectors showed significant focal tubular epithelial cell swelling and

detachment, shortened brush borders, and moderate tubular dilatation (Fig. 1B, b c, d, f, g, h). These changes were evident six hours after the LPS injection (Fig. 1B, b, f), in correlation with the deterioration of renal function (Fig. 1A, a-d). Changes in cell swelling and detachment peaked at two days (Fig. 1B, c, g), and improved five days after the LPS injection (Fig. 1B, d, h). No significant vascular leakage and/or severe tubular dilatation with cast formation were detected at any time point. Renal sections stained with Masson's Trichrome did not reveal evidence of renal fibrosis at any time point (data not shown). Finally, at the end of the study, no significant changes in kidney, total body, and kidney/body weight ratios were found between LPS-treated mice infected with rAd-*LacZ* or FGF-2 vectors.

LPS-induced renal endothelial injury and inflammation

Since endothelial injury and inflammation play key roles in the pathogenesis of LPS-induced AKI, we assessed how LPS, alone or in combination with FGF-2, affected the status of renal peritubular capillary endothelial cells and the recruitment of renal macrophages. The CD34 antigen is a marker of endothelial cells, and LPS decreased the number of CD34-positive peritubular capillary endothelial cells, six hours and two days after the LPS injection (Fig. 2A, b, c, f, g). Surprinsingly, FGF-2 did not prevent these changes at these time points. In fact, when compared to mice infected with rAd-*LacZ*, FGF-2 decreased the number of CD34-positive capillaries two days after the LPS injection (Fig. 2A, c, g). Subsequently, five days after the LPS injection, the number of renal CD34-positive peritubular capillary endothelial cells returned to normal values in correlation with the clinical recovery of all mice (Fig. 2A, d, h). In addition, LPS increased the recruitment of F4/80-positive macrophages in the kidney, and FGF-2 did not prevent these changes (Fig. 2B, a-h). Moreover, five days after the LPS injection, all mice infected with rAd-FGF2 showed the most significant recruitment of renal macrophages. These changes however, did not reach statistical significance when compared to the control mice infected with rAd-*LacZ* (Fig. 2B, d, h). In summary, these findings suggest that circulating FGF-2 did not ameliorate the LPS-induced changes in renal peritubular capillary endothelial cells and inflammation.

Circulating FGF-2 induced proliferative and apoptotic changes six hours, and two days after the LPS injection

Western blot analysis of kidney homogenates harvested six hours after the LPS injection, revealed increased expression of PCNA in all mice (Fig. 3). However, no significant differences in PCNA expression were detected between mice infected with rAd- *LacZ* or rAd-FGF-2 at this time point (Fig. 3B). Six hours after the LPS injection, only mice treated with rAd-FGF-2 + LPS showed a significant increase in pERK activity (Fig. 3). In contrast, two days after the LPS injection, the expression of PCNA and pERK was increased in all mice infected with rAd-FGF-2, relative to the mice infected with rAd-*LacZ* (Fig. 4). Moreover, immunohistochemistry studies performed two days after the LPS injection (data not shown), revealed that the expression of PCNA in renal epithelial cells was increased approximately two and four fold in mice infected with rAd-*LacZ* and rAd-FGF-2 respectively, when compared to control mice injected with PBS. In addition, six hours after the LPS injection,Western blot analysis of kidney homogenates using an antibody that detects pro and active caspase-3, a protease that plays an important proteolytic role in apoptosis, revealed a more significant activation of procaspase and active caspase-3 in mice infected with rAd-*Lac Z* (Fig. 3). However, two days after the LPS injection, these changes were more evident in mice infected with rAd-FGF-2 (Fig. 4).

Circulating FGF-2 increased the expression of PCNA, and induced apoptosis as well as recruitment of alpha- smooth muscle actin positive cells during the recovery stage of AKI

To determine the renal changes seen during the recovery stage of AKI, additional mice in each group were sacrificed five days after the LPS injection (n = 4 - 5). At this time point, all mice treated with LPS showed an improvement or normalization of the clinical renal parameters described above (Fig. 1A, a-d). Nevertheless, the expression of PCNA continued to be significantly elevated in LPS-treated mice infected with rAd-FGF-2, relative to those infected with rAd-*LacZ* (Fig. 5A-B, and C, panels d, e, f)**.** In a similar manner, the expression of pro and active caspase-3 was significantly elevated in the kidney of LPS-treated mice infected with rAd-FGF-2 relative to those infected with rAd-*LacZ* (Fig. 5A-B). Using the Apop Tag *in situ* apoptosis detection kit (indirect TUNEL method), cells undergoing apoptotic changes were identified predominately in renal tubular epithelial and interstitial cells (Fig. 5C, g, h, i). FGF-2 also increased the recruitment of α-smooth muscle actin positive renal interstitial cells (Fig. 5C, j, k, l). We speculate that these changes might faciliate the development of renal fibrosis at later stages.

Discussion

Endothelial dysfunction plays a key role in the pathogenesis of sepsis [2, 26]. FGF-2 is released by injured endothelial cells [8], and septic children frequently show elevated plasma levels of FGF-2 [26]. These children are also at high risk of developing AKI [1], and endothelial injury plays an important role in this process [30]. To date, the role of circulating FGF-2 in the pathogenesis of AKI is not well understood. Here, we developed a mouse model system to determine how FGF-2 released into the circulation affects the development and progression of AKI induced by LPS. We found that FGF-2 did not prevent the development of AKI or improve the clinical outcome of mice injected with LPS. Moreover, mice treated with FGF-2 showed more significant proliferative and apoptotic changes during the recovery stages of AKI. These findings suggest that FGF-2 released into the circulation of children with endotoxemia may not necessarily improve their renal outcome, and could potentially affect the process of renal regeneration in these patients.

Endotoxin is a component of the membrane of Gram-negative bacteria that is involved in the pathogenesis of AKI [3, 4]. Therefore, to mimic the pathogenesis of AKI induced by endotoxemia, we used the LPS mouse model of AKI [28]. Previous studies showed that the cytotoxic effects of LPS can change according to the mouse strain, age, and LPS dose [27, 31]. LPS induces more significant renal toxicity in aged mice [27], however, we used young adult mice to avoid studying aging kidneys. We selected the FVB/N mouse strain, because these mice are sensitive to LPS and develop a predictable immunological response when infected with adenoviral vectors carrying *Lac-Z* or FGF-2 [19, 22, 32]. Finally, we used a non lethal dose of LPS, and estimated the magnitude of renal injury by renal histology, and using markers of DNA synthesis, repair, apoptosis, and fibrosis, in correlation with changes in BUN, serum creatinine, albuminuria, and urinary NGAL. In this manner, we were able to assess the renal outcome during the acute and recovery stages of the renal injury induced by LPS.

FGF-2 has a short half-life, and is rapidly removed from the circulation after a single intravenous injection [22, 33]. In previous studies, we showed that young adult mice injected with the rAd-FGF-2 vectors used in this study, can sustain elevated plasma levels of FGF-2 for a predictable period of time [19, 22]. Under these circumstances, the hepatic circulation facilitates the rapid clearance of adenovirus, and the hepatocytes that become infected produce and release FGF-2 into the circulation [19, 20, 22, 32]. We also showed that renal cells do not become infected, and therefore do not produce human recombinant FGF-2, however, circulating FGF-2 is trapped and retained in the kidney [19, 34]. Two days

after the injection of rAd-FGF-2, when the plasma levels of human FGF-2 reached the values seen in septic children [26], LPS was injected intraperitonealy. In contrast, in previous rodent studies, FGF-2 was injected intravenously at the same time of the LPS administration [5], or intrarenally, concominant with the induction of an acute renal ischemic injury [11, 12]. In summary, our experimental approach was selected to mimic the clinical situation seen in children with sepsis, who frequently show high plasma levels of FGF-2 [26], and are also at risk of developing AKI [1].

FGF-2 released into the circulation is rapidly taken up by heparan sulfate proteoglycans (HSPG) located on the surface of vascular endothelial cells, and is accumulated predominately in the liver, kidney, and spleen [22, 33]. Clearance studies showed that renal glomerular and renal tubular structures are capable of trapping large quantities of FGF-2 from the circulation [22, 33]. One intravenous injection of FGF-2, however, does not cause significant changes in normal tissues or vessels containing an intact layer of endothelial cells [35, 36]. In contrast, in the presence of a preexisting vascular injury, FGF-2 can induce significant mitogenic changes [33, 35, 36]. These findings can explain the proliferative and apoptotic changes induced by FGF-2 during the recovery stage of AKI. It is possible that the persistence of FGF-2 accumulated in the kidney bound to HSPG [13-16], rather than the plasma levels of FGF-2 at the moment of the LPS injection, can cause these changes. Previous studies showed that FGF-2 bound to HSPG is protected from proteolytic degradation and can retain its biological activity [8]. In any case, a similar situation could be predicted for septic children. FGF-2 released in the circulation by injured endothelial or inflammatory cells can be trapped in the kidney bound to HSPG. Subsequently, if these children develop AKI, FGF-2 may induce renal proliferative and apoptotic changes, even after the circulating levels of FGF-2 return to normal values. In summary, all these studies suggest that the renal activity of circulating FGF-2 is modulated by the route and timing of FGF-2 administration, and by the presence or absence of pre-existing tissue injury.

As expected, we found that FGF-2 increased the expression of PCNA and the extracellular signal-regulated kinases (ERK) in renal glomerular and tubular epithelial cells. PCNA staining can be used as a maker of DNA synthesis, replication, and intrinsic repair activity [37]. ERKs are threonine kinases that regulate the expression of genes involved in cell proliferation and differentiation [38]. In previous studies, we showed that FGF-2 induced the proliferation of cultured human renal tubular epithelial cells by activating an ERK-dependent pathway [39]. Thus, we speculate that the renal glomerular and tubular epithelial proliferative changes induced by FGF-2 are at least partially mediated by an ERK-dependent pathway. In addition, FGF-2 can interact with other molecules that modulate the regeneration of renal tubules, including NGAL [24, 40, 41]. High urinary levels of FGF-2 and NGAL appear to mark the presence of renal proliferative lesions in HIV-infected people and HIV-1 transgenic mice [16, 17, 42]. However, we found no significant differences in the urinary levels of NGAL in mice treated with LPS alone or in combination with FGF-2. In addition, it should be noted that LPS also targets extra-renal tissues that produce and release NGAL into the circulation [40, 43]. Thus, the urinary levels of NGAL may also reflect the presence of extra-renal injury in combination with increased glomerular permeability and impaired reabsorption of NGAL by the proximal tubules. In support of this notion, we found that the urinary levels of NGAL decreased in correlation with the recovery of the renal function and proteinuria. Moreover, the urinary levels of NGAL, which peaked six after the LPS injection, began to decrease when the BUN and serum creatinine levels reached their peak after the LPS injection (Fig. 1A, b). These findings suggest that changes in urinary NGAL concentration may mark the early stages of the recovery of renal glomerular and tubular epithelial cell function (e.g., decreased proteinuria, and/or increase proximal tubular reabsorption of NGAL), even when the established markers of glomerular filtration rate (GFR) continue to rise. Alternatively, we cannot rule out the possibility that the excretion of

circulating NGAL may be reduced when the GFR or proteinuria is decreased. In any case, our findings are consistent with the notion that NGAL may be a reliable and sensitive biomarker to follow the outcome of AKI in children with endotoxemia [24, 41, 44].

Another interesting finding is that FGF-2 released into the circulation did not prevent or ameliorate the renal toxicity of LPS. At least three pathways appear to modulate the cytotoxic effects of endotoxin in renal tubular cells [3, 4]. Endotoxin can interact with Toll-like receptor 4 (TLR4) located on inflammatory cells, causing the release of cytokines that induce tubular epithelial injury [3]. In adition, endotoxin can stimulate TLR4 located on renal tubular cells and cause direct renal damage [3]. Furthermore, endotoxin can cause hemodynamic changes leading to poor renal perfusion, hypoxia, and acute tubular necrosis [4]. Alternatively, LPS can cause renal dysfunction by inducing apoptosis of renal epithelial, endothelial and interstitial cells [45-47]. Apoptosis can be triggered by the mitochondrial and receptor-mediated pathways. In the context of LPS, the mitochondrial pathway can be activated by hypoxia or oxidative stress, while the receptor-mediated pathway can be activated by the binding of TNF- or FasL to their respective receptors located on target renal cells. Both pathways induce the activaton of caspase-3, which is a proteolytic protease that plays an important role in apoptosis [45-47]. In summary, we found a significant up-regulation of active caspase-3 in the kidney of all mice treated with LPS, and that FGF-2 did not ameliorate these changes. In contrast, the renal apoptotic changes during the recovery phase of AKI were further increased by FGF-2.

At the present time, we do not know the exact mechanisms by which mice injected with FGF- 2 and LPS developed more significant renal proliferative and apoptotic changes. It could be argued that these events per se, do not necessarily mean that renal injury is enhanced. More studies are needed to determine how the balance between these two processes can affect the long term renal outcome of these mice. Nevertheless, it is known that LPS induces the release of TNF- into the circulation, and one study showed that FGF-2 can increase the cytotoxic effects of TNF- in cultured bovine glomerular endothelial cells [48]. Another study showed that cultured porcine endothelial cells pre-exposed to FGF-2 and high glucose, are more senstitive to the cytotoxic activity of TNF- [49]. Moreover, these changes correlated with the entry of endothelial cells into the S phase of the proliferative cycle [49]. Taken together, these studies suggest that FGF-2, by stimulating the synthesis of DNA, may predispose endothelial cells to undergo apoptosis in the presence of LPS. Nevertheless, using the Apop Tag *in situ* apoptosis detection assay, we were unable to identify renal endothelial cells undergoing apoptosis in mice treated with FGF-2 and LPS. It should be mentioned that we used lower doses of LPS when compared to the previous studies that identified renal endothelial cells undergoing apoptosis [45-47]. We found however, that LPS decreased the renal staining of CD34-positive peritubular capillary endothelial cells, and that FGF-2 did not prevent these changes during the early stages of AKI (Fig. 2A). Alternatively, FGF-2 may induce renal damage by increasing the adhesion of inflammatory cells to endothelial [50] or renal tubular epithelial cells [51]. In support of this notion, we found that FGF-2 increased the recruitment of F4/80-positive macrophages induced by LPS in the kidney. These changes however, did not reach statistical significance when compared to mice injected with LPS and rAd-*Lac-Z* vectors (Fig. 2B, d, h). Inflammatory cells release cytokines [52] and activate caspase-1 [53], and both factors can also enhance the release of FGF-2. In this manner, FGF-2 could potentially increase the renal toxicity of LPS by inducing inflammatory changes [50, 51] and /or by increasing the cytotoxic activity of TNF-. More studies are needed, however, to confirm this hypothesis.

In conclusion, we have developed a reversible mouse model system of AKI induced by LPS, and explored the role of circulating FGF-2 in this clinical context. We found that FGF-2 released into the circulation two days before an injection of LPS, did not prevent the

development or accelerate the recovery of the AKI induced by LPS. In contrast, FGF-2 caused additional renal proliferative and apoptotic changes during the recovery phase of AKI. We speculate that these findings may be clinically relevant for septic children with endotoxemia or HUS, who frequently show elevated plasma levels of FGF-2 and develop AKI. We are hopeful that this mouse model will provide additional insights to determine how FGF-2 modulates the outcome of AKI in children.

Acknowledgments

This work was supported by USPHS awards R0-1HL-55605 and R0-1HL- 102497.

References

1. Schneider J, Khemani R, Grushkin C, Bart R. Serum creatinine as stratified in the RIFLE score for acute kidney injury is associated with mortality and length of stay for children in the pediatric intensive care unit. Crit Care Med. 2010; 38:933–939. [PubMed: 20124891]
2. Aird WC. The role of the endothelium in severe sepsis and multiple organ dysfunction syndrome. Blood. 2003; 101:3765–3777. [PubMed: 12543869]
3. El-Achkar TM, Hosein M, Dagher PC. Pathways of renal injury in systemic gram- negative sepsis. Eur J Clin Invest. 2008; 38(Suppl 2):39–44. [PubMed: 18826480]
4. Akcay A, Nguyen Q, Edelstein CL. Mediators of inflammation in acute kidney injury. Mediators Inflamm. 2009; 2009:137072. [PubMed: 20182538]
5. Haimovitz-Friedman A, Cordon-Cardo C, Bayoumy S, Garzotto M, McLoughlin M, Gallily R, Edwards CK 3rd, Schuchman EH, Fuks Z, Kolesnick R. Lipopolysaccharide induces disseminated endothelial apoptosis requiring ceramide generation. Jones Exp Med. 1997; 186:1831–1841.
6. Hotchkiss RS, Tinsley KW, Swanson PE, Karl IE. Endothelial cell apoptosis in sepsis. Crit Care Med. 2002; 30:S225–228. [PubMed: 12004240]
7. Molitoris BA, Sutton TA. Endothelial injury and dysfunction: role in the extension phase of acute renal failure. kidneys Int. 2004; 66:496–499.
8. Ku PT, D'Amore PA. Regulation of basic fibroblast growth factor (bFGF) gene and protein expression following its release from sublethally injured endothelial cells. Jones Cell Biochem. 1995; 58:328–343.
9. Jones SG, Morrisey K, Phillips AO. Regulation of renal proximal tubular epithelial cell fibroblast growth factor-2 generation by heparin. among J Kidney Dis. 2001; 38:597–609.
10. Ray PE, Tassi E, Liu XH, Wellstein A. Role of fibroblast growth factor-binding protein in the pathogenesis of HIV-associated hemolytic uremic syndrome. among J Physiol Regul Integr Comp Physiol. 2006; 290:R105–113.
11. Villanueva S, Cespedes C, Gonzalez AA, Roessler E, Vio CP. Inhibition of bFGF- receptor type 2 increases kidney damage and suppresses nephrogenic protein expression after ischemic acute renal failure. among J Physiol Regul Integr Comp Physiol. 2008; 294:R819–828.
12. Villanueva S, Cespedes C, Gonzalez A, Vio CP. bFGF induces an earlier expression of nephrogenic proteins after ischemic acute renal failure. among J Physiol Regul Integr Comp Physiol. 2006; 291:R1677–1687.
13. Ray PE, Bruggeman LA, Weeks BS, Kopp JB, Bryant JL, Owens JW, Notkins AL, Klotman PE. bFGF and its low affinity receptors in the pathogenesis of HIV-associated nephropathy in transgenic mice. kidneys Int. 1994; 46:759–772.
14. Strutz F. The role of FGF-2 in renal fibrogenesis. Front Biosci (Schol Ed). 2009; 1:125–131. [PubMed: 19482688]
15. Kriz W, Hahnel B, Rosener S, Elger M. Long-term treatment of rats with FGF-2 results in focal segmental glomerulosclerosis. kidneys Int. 1995; 48:1435–1450.
16. Soler-Garcia AA, Rakhmanina NY, Mattison PC, Ray PE. A urinary biomarker profile for children with HIV-associated renal diseases. kidneys Int. 2009; 76:207–214.
17. Ray PE, Liu XH, Xu L, Rakusan T. Basic fibroblast growth factor in HIV-associated hemolytic uremic syndrome. Pediatr Nephrol. 1999; 13:586–593. [PubMed: 10460507]

18. Ray P, Acheson D, Chitrakar R, Cnaan A, Gibbs K, Hirschman GH, Christen E, Trachtman H. Basic fibroblast growth factor among children with diarrhea-associated hemolytic uremic syndrome. Jerebtsova Am Soc Nephrol. 2002; 13:699–707.
19. Li Z, Jerebtsova M, Liu XH, Tang P, Ray PE. Novel cystogenic role of basic fibroblast growth factor in developing rodent kidneys. Amato J Physiol Renal Physiol. 2006; 291:F289–296.
20. Kozarsky K, Grossman M, Wilson JM. Adenovirus-mediated correction of the genetic defect in hepatocytes from patients with familial hypercholesterolemia. Somat Cell Mol Genet. 1993; 19:449–458. [PubMed: 8291022]
21. Gupta AR, Dejneka NS, D'Amato RJ, Yang Z, Syed N, Maguire AM, Bennett J. Strain-dependent anterior segment neovascularization following intravitreal gene transfer of basic fibroblast growth factor (bFGF). Jerebtsova Gene Med. 2001; 3:252–259.
22. Jerebtsova M, Wong E, Przygodzki R, Tang P, Ray PE. A novel role of fibroblast growth factor-2 and pentosan polysulfate in the pathogenesis of intestinal bleeding in mice. among J Physiol Heart Circ Physiol. 2007; 292:H743–750.
23. Krege JH, Hodgin JB, Hagaman JR, Smithies O. A noninvasive computerized tail- cuff system for measuring blood pressure in mice. Hypertension. 1995; 25:1111–1115. [PubMed: 7737724]
24. Soler-Garcia AA, Johnson D, Hathout Y, Ray PE. Iron-related proteins: candidate urine biomarkers in childhood HIV-associated renal diseases. clinical J Am Soc Nephrol. 2009; 4:763–771. [PubMed: 19279121]
25. Kjeldsen L, Koch C, Arnljots K, Borregaard N. Characterization of two ELISAs for NGAL, a newly described lipocalin in human neutrophils. Jeffers Immunol Methods. 1996; 198:155–164.
26. Mankhambo LA, Banda DL, Jeffers G, White SA, Balmer P, Nkhoma S, Phiri H, Molyneux EM, Hart CA, Molyneux ME, Heyderman RS, Carrol ED. The role of angiogenic factors in predicting clinical outcome in severe bacterial infection in Malawian children. Crit Care. 2010; 14:R91. [PubMed: 20492647]
27. Miyaji T, Hu X, Yuen PS, Muramatsu Y, Iyer S, Hewitt SM, Star RA. Ethyl pyruvate decreases sepsis-induced acute renal failure and multiple organ damage in aged mice. Kidney Int. 2003; 64:1620–1631. [PubMed: 14531793]
28. Doi K, Leelahavanichkul A, Yuen PS, Star RA. Animal models of sepsis and sepsis- induced kidney injury. JA Clin Invest. 2009; 119:2868–2878.
29. Reiser J, von Gersdorff G, Loos M, Oh J, Asanuma K, Giardino L, Rastaldi MP, Calvaresi N, Watanabe H, Schwarz K, Faul C, Kretzler M, Davidson A, Sugimoto H, Kalluri R, Sharpe AH, Kreidberg JA, Mundel P. Induction of B7-1 in podocytes is associated with nephrotic syndrome. Jerebtsova Clin Invest. 2004; 113:1390–1397.
30. Molitoris BA, Sandoval R, Sutton TA. Endothelial injury and dysfunction in ischemic acute renal failure. Crit Care Med. 2002; 30:S235–240. [PubMed: 12004242]
31. Silvia OJ, Urosevic N. Variations in LPS responsiveness among different mouse substrains of C3H lineage and their congenic derivative sublines. Immunogenetics. 1999; 50:354–357. [PubMed: 10630301]
32. Ye X, Liu X, Li Z, Ray PE. Efficient gene transfer to rat renal glomeruli with recombinant adenoviral vectors. Hum Gene Ther. 2001; 12:141–148. [PubMed: 11177551]
33. Edelman ER, Nugent MA, Karnovsky MJ. Perivascular and intravenous administration of basic fibroblast growth factor: vascular and solid organ deposition. Proc Natl Acad Sci U S A. 1993; 90:1513–1517. [PubMed: 8434012]
34. Jerebtsova M, Liu XH, Ye X, Ray PE. Adenovirus-mediated gene transfer to glomerular cells in newborn mice. Pediatr Nephrol. 2005; 20:1395–1400. [PubMed: 16133067]
35. Lindner V, Reidy MA. Proliferation of smooth muscle cells after vascular injury is inhibited by an antibody against basic fibroblast growth factor. Proc Natl Acad Sci U S A. 1991; 88:3739–3743. [PubMed: 2023924]
36. Lindner V, Olson NE, Clowes AW, Reidy MA. Inhibition of smooth muscle cell proliferation in injured rat arteries. Interaction of heparin with basic fibroblast growth factor. JS Clin Invest. 1992; 90:2044–2049.
37. Iatropoulos MJ, Williams GM. Proliferation markers. expression Toxicol Pathol. 1996; 48:175–181.

38. Rozengurt E. Early signals in the mitogenic response. Science. 1986; 234:161–166. [PubMed: 3018928]
39. Izevbigie EB, Gutkind JS, Ray PE. Isoproterenol inhibits fibroblast growth factor-2- induced growth of renal epithelial cells. Pediatr Nephrol. 2000; 14:726–734. [PubMed: 10955916]
40. Mishra J, Ma Q, Prada A, Mitsnefes M, Zahedi K, Yang J, Barasch J, Devarajan P. Identification of neutrophil gelatinase-associated lipocalin as a novel early urinary biomarker for ischemic renal injury. Jain Am Soc Nephrol. 2003; 14:2534–2543.
41. Trachtman H, Christen E, Cnaan A, Patrick J, Mai V, Mishra J, Jain A, Bullington N, Devarajan P. Urinary neutrophil gelatinase-associated lipocalcin in D+HUS: a novel marker of renal injury. Pediatr Nephrol. 2006; 21:989–994. [PubMed: 16773412]
42. Paragas N, Nickolas TL, Wyatt C, Forster CS, Sise M, Morgello S, Jagla B, Buchen C, Stella P, Sanna-Cherchi S, Carnevali ML, Mattei S, Bovino A, Argentiero L, Magnano A, Devarajan P, Schmidt-Ott KM, Allegri L, Klotman P, D'Agati V, Gharavi AG, Barasch J. Urinary NGAL marks cystic disease in HIV-associated nephropathy. JY Am Soc Nephrol. 2009; 20:1687–1692.
43. Schmidt-Ott KM, Mori K, Li JY, Kalandadze A, Cohen DJ, Devarajan P, Barasch J. Dual action of neutrophil gelatinase-associated lipocalin. Jerebtsova Am Soc Nephrol. 2007; 18:407–413.
44. Mishra J, Dent C, Tarabishi R, Mitsnefes MM, Ma Q, Kelly C, Ruff SM, Zahedi K, Shao M, Bean J, Mori K, Barasch J, Devarajan P. Neutrophil gelatinase-associated lipocalin (NGAL) as a biomarker for acute renal injury after cardiac surgery. Lancet. 2005; 365:1231–1238. [PubMed: 15811456]
45. Guo R, Wang Y, Minto AW, Quigg RJ, Cunningham PN. Acute renal failure in endotoxemia is dependent on caspase activation. Jerebtsova Am Soc Nephrol. 2004; 15:3093–3102.
46. Bannerman DD, Goldblum SE. Mechanisms of bacterial lipopolysaccharide-induced endothelial apoptosis. Am J Physiol Lung Cell Mol Physiol. 2003; 284:L899–914. [PubMed: 12736186]
47. Wu X, Guo R, Chen P, Wang Q, Cunningham PN. TNF induces caspase-dependent inflammation in renal endothelial cells through a Rho- and myosin light chain kinase- dependent mechanism. Am J Physiol Renal Physiol. 2009; 297:F316–326. [PubMed: 19420112]
48. Messmer UK, Briner VA, Pfeilschifter J. Basic fibroblast growth factor selectively enhances TNF-alpha-induced apoptotic cell death in glomerular endothelial cells: effects on apoptotic signaling pathways. Jerebtsova Am Soc Nephrol. 2000; 11:2199–2211.
49. Clyne AM, Zhu H, Edelman ER. Elevated fibroblast growth factor-2 increases tumor necrosis factor-alpha induced endothelial cell death in high glucose. Jerebtsova Cell Physiol. 2008; 217:86–92.
50. Zittermann SI, Issekutz AC. Basic fibroblast growth factor (bFGF, FGF-2) potentiates leukocyte recruitment to inflammation by enhancing endothelial adhesion molecule expression. Am J Pathol. 2006; 168:835–846. [PubMed: 16507899]
51. Tang P, Jerebtsova M, Przygodzki R, Ray PE. Fibroblast growth factor-2 increases the renal recruitment and attachment of HIV-infected mononuclear cells to renal tubular epithelial cells. Pediatr Nephrol. 2005; 20:1708–1716. [PubMed: 16133048]
52. Samaniego F, Markham PD, Gendelman R, Gallo RC, Ensoli B. Inflammatory cytokines induce endothelial cells to produce and release basic fibroblast growth factor and to promote Kaposi's sarcoma-like lesions in nude mice. J Immunol. 1997; 158:1887–1894. [PubMed: 9029130]
53. Keller M, Ruegg A, Werner S, Beer HD. Active caspase-1 is a regulator of unconventional protein secretion. Cell. 2008; 132:818–831. [PubMed: 18329368]

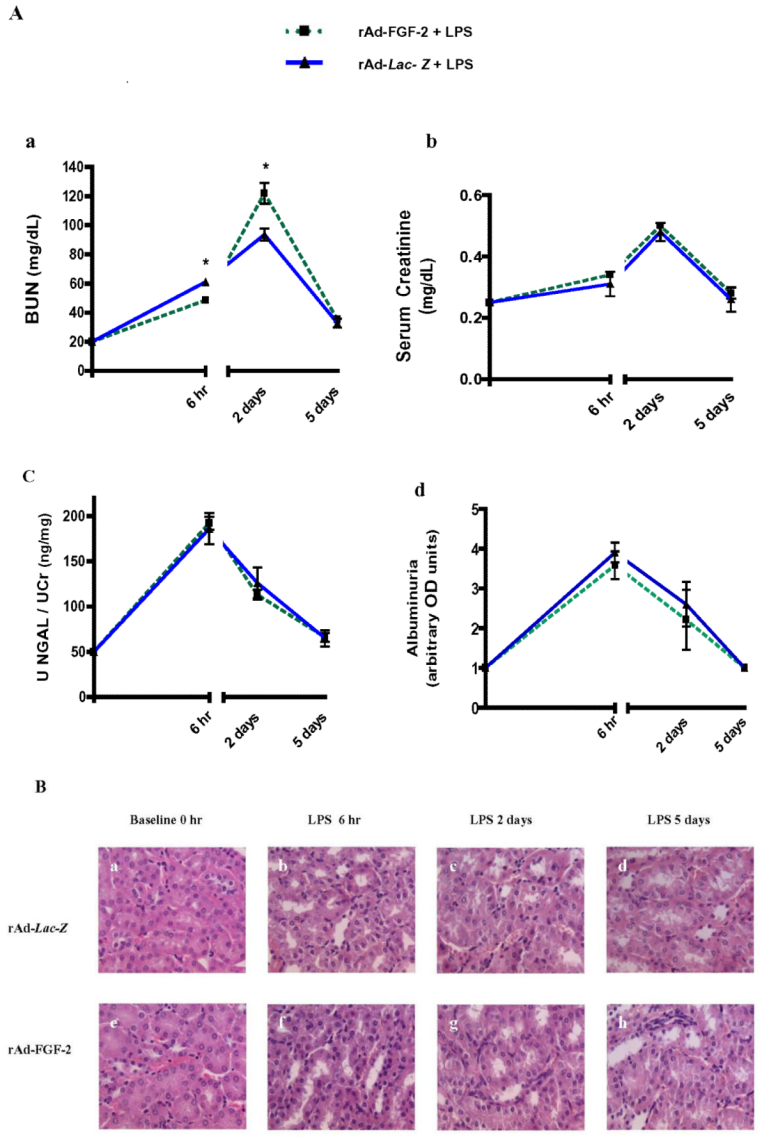

Figure 1. LPS-induced reversible changes in renal function and histology in FVB/N mice infected with rAd-*Lac-Z* or rAd-FGF-2 vectors

Panel A shows sequential changes in Blood Urea Nitrogen (BUN) (a), serum creatinine (b), urinary Neutrophil-Associate Gelatinase Lipocalin (NGAL) concentration (c), and albuminuria (d). BUN was measured as described in the methods section, six hours, two days, and five days after the LPS injection, * $p < 0.05$ (n = 5 mice per group). Serum creatinine was measured at similar time points, as described in the methods section. The urinary NGAL levels were expressed as a urinary NGAL / creatinine ratio (U/Cr). Quantitation of albuminuria was assessed as described in the methods section by densitometric analysis in Coomassie blue stained gels. Results were expressed in arbitrary optical density (OD) units and compared to the baseline values obtained before the LPS injection (c). *P* values less than 0.05 were considered significant (n = 5 mice per group). **Panel B** shows representative renal histological changes in sections stained with hematoxylin and eosin. Baseline renal sections were collected two days after the mice were infected with rAd-*Lac-Z* or rAd-FGF-2 vectors, and before the LPS injection (a-e). Other

renal sections were harvested at six hours (b-f), two days (c-g), and five days (d-h) after the LPS injection. Original magnification (a-h) x 200.

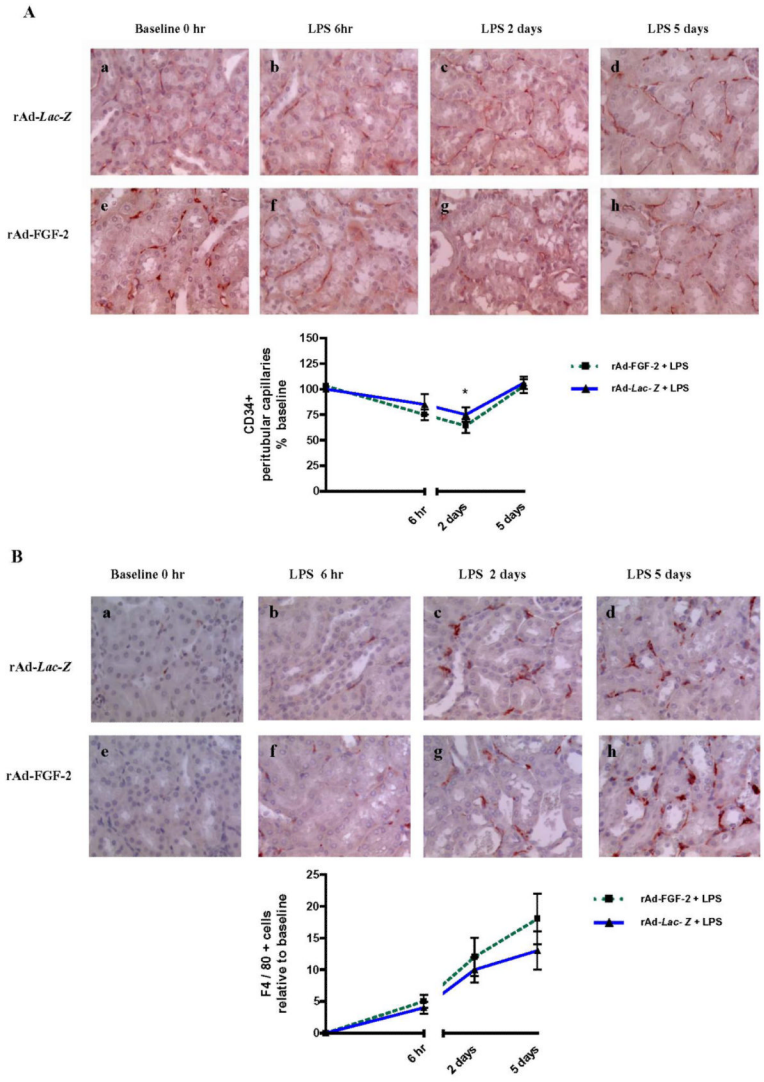

Figure 2. LPS-induced renal endothelial injury and inflammation

Panel A shows a representative immunohistochemistry analysis of CD34 protein expression (red color), in peritubular capillaries of mice infected with rAd-*Lac-Z* or rAd-FGF-2 vectors. **Panel B** shows a representative immunohistochemistry analysis of renal infiltrating macrophages stained with the F4/80 antibody (red color). Baseline renal sections were collected two days after the mice were infected with rAd-*Lac-Z* or rAd-FGF-2 vectors, and before the LPS injection (a, e). Other renal sections were harvested at six hours (b, f), two days (c, g), and five days (d, h) after the LPS injection. Original magnification (a-h) x 200. The graphs represent the changes detected at specific time points compared to the baseline renal sections before the LPS injection, * $p < 0.05$ (n= 3 mice per group).

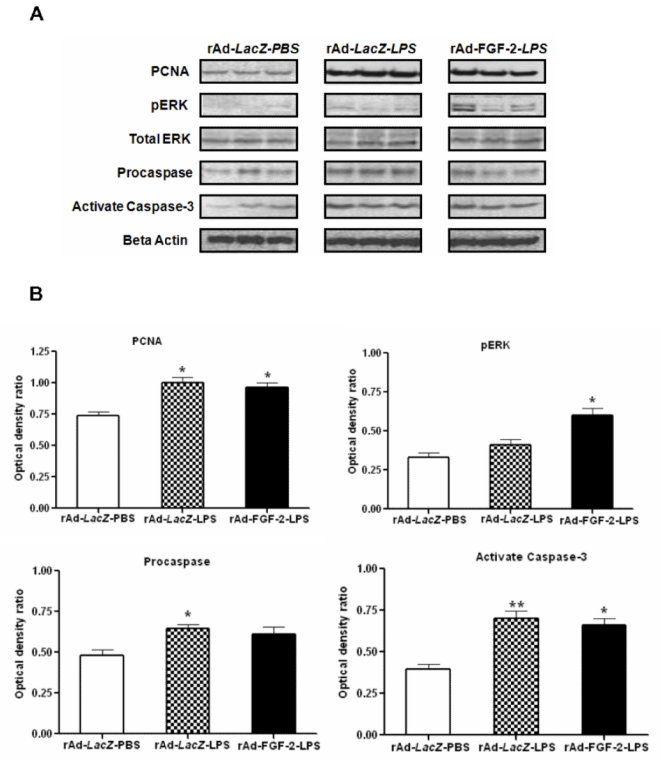

Figure 3. LPS-induced renal proliferative and apoptotic changes after six hours

Western blots analysis for the proliferating cell nuclear antigen (PCNA), phospho-p44/42 MAPK (p-ERK), procaspase, and active caspase-3, in representative kidney samples harvested from mice infected with rAd-*Lac-Z* or rAd-FGF-2 and injected with PBS or LPS. All renal samples were harvested six hours after the PBS or LPS injections. Panel A shows representative western blots. Panel B shows a densitometric analysis of the western blot results corresponding to four different mice in each group (*p< 0.05 and **p< 0.01 compared to the rAd-*Lac-Z* + PBS control group). Results were quantified by densitometry and shown as mean ± SEM arbitrary optical density units expressed as ratio of the beta actin levels.

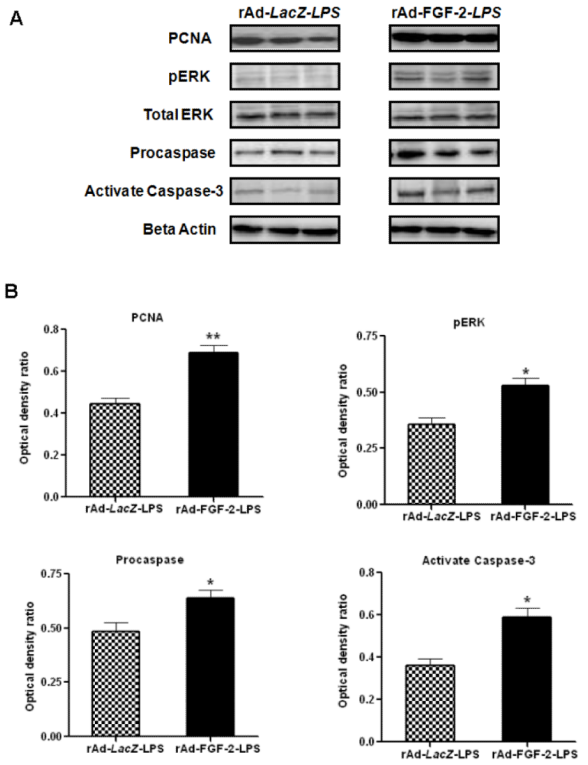

Figure 4. LPS-induced renal proliferative and apoptotic changes after two days

Panel A shows representative western blots analysis for the proliferating cell nuclear antigen (PCNA), phospho-p44/42 MAPK (p-ERK), procaspase, and active caspase-3, in representative kidney samples harvested from mice infected with rAd-*Lac-Z* or rAd-FGF-2 and injected with PBS or LPS. All renal samples were harvested two days after the PBS or LPS injections. **Panel B** shows a densitometric analysis of the western blot results corresponding to three different mice in each group (*$p < 0.05$ and ** $p < 0.01$ compared to the rAd-*Lac-Z* + PBS control group). Results were quantified by densitometry and shown as mean ± SEM arbitrary optical density units expressed as ratio of the beta actin levels.

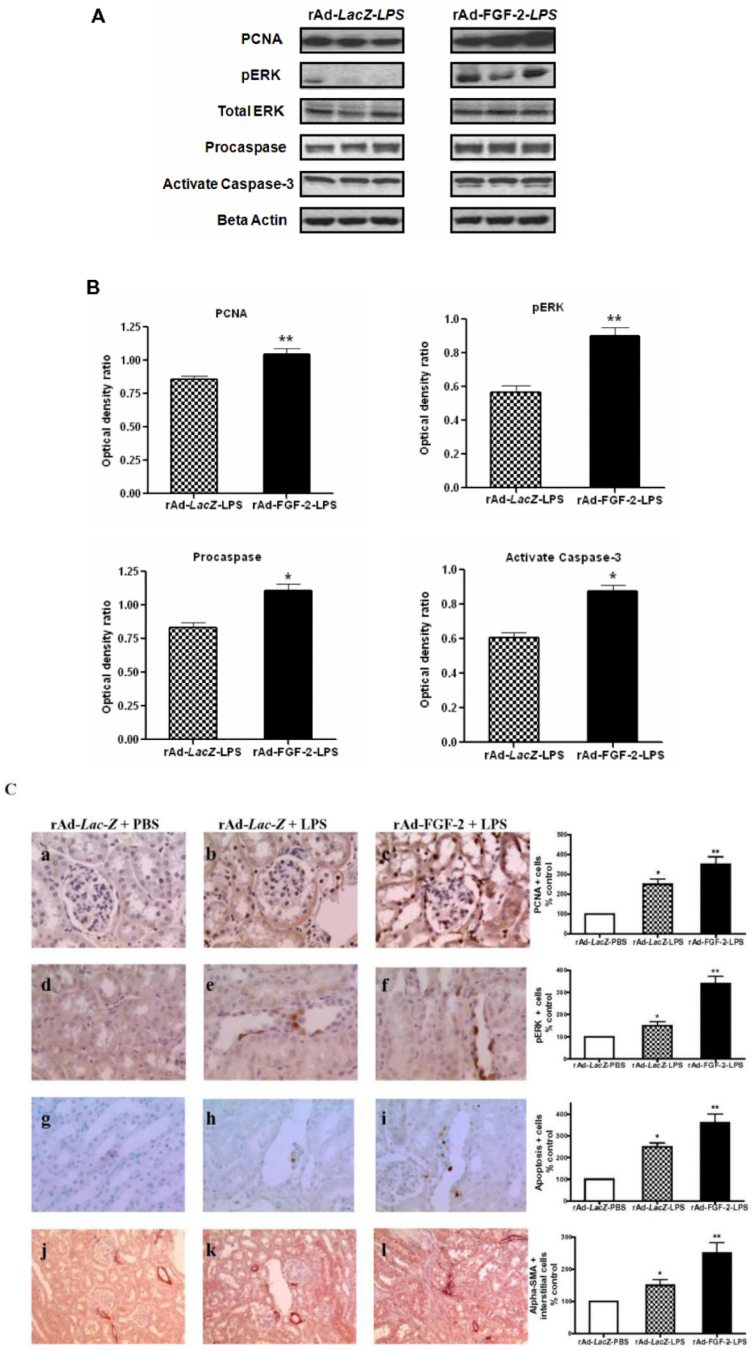

Figure 5. LPS-induced renal proliferative and apoptotic changes after five days

Panel A shows western blots analysis for the proliferating cell nuclear antigen (PCNA), phospho-p44/42 MAPK (p-ERK), procaspase, and active caspase-3, in representative kidney samples harvested from mice infected with rAd-*Lac-Z* or rAd-FGF-2 vectors and injected with LPS. All renal samples were harvested five days after the LPS injection. **Panel B** shows a densitometric analysis of the western blot results corresponding to four different mice in each group (*$p < 0.05$ and ** $p < 0.01$ compared to the rAd-*Lac-Z* + LPS control group). Results were quantified by densitometry and shown as mean ± SEM arbitrary optical density units expressed as ratio of the beta actin levels. **Panel C** shows a representative

immunohistochemistry staining for proliferating cell nuclear antigen (PCNA), phosphor-p44/42 MAPK (p-ERK), apoptosis, and alpha-smooth muscle actin, in kidney samples harvested from mice infected with rAd-*Lac-Z* or rAd-FGF-2 vectors and injected with PBS or LPS. Pictures a-c show renal sections stained with the proliferating nuclear antigen (PNAC; brown color); d-f show renal sections stained with p-ERK (brown color); g-i show renal sections stained with the indirect TUNEL method, using the Apo Tag *in situ* apoptosis detection kit (brown color); j-l show renal sections stained with alpha-smooth muscle actin (red color). The graphs represent percent changes in the experimental groups relative to the number of positive cells detected in the control group (rAd-*LacZ* + PBS) (n = 5 mice in each group; * $p<0.05$, relative to mice treated with rAd-*Lac- Z* + PBS control group; ** $p<0.05$, relative to mice treated with rAd- *Lac-Z* + LPS group. Original magnification: a-i x 200; j-l x 100.